Global Change Biology (2007) **13,** 2218–2229, doi: 10.1111/j.1365-2486.2007.01416.x

Effects of an induced drought on soil carbon dioxide (CO_2) efflux and soil CO_2 production in an Eastern Amazonian rainforest, Brazil

ELENEIDE DOFF SOTTA*, EDZO VELDKAMP*, LUITGARD SCHWENDENMANN†, BRENDA ROCHA GUIMARÃES‡, ROSIENE KEILA PAIXÃO‡, MARIA DE LOURDES P. RUIVO‡, ANTONIO CARLOS LOLA DA COSTA¶ and PATRICK MEIR§

Institute of Soil Science and Forest Nutrition, University of Göttingen, Büsgenweg 2, D-37077, Göttingen, Germany, †Institute of Silviculture, University of Göttingen, Büsgenweg 1, D-37077, Göttingen, Germany, ‡Museu Paraense Emilio Goeldi – Campus de Pesquisa, Coordenacao de Ciencias da Terra e Ecologia. TerraFirme, Av. Perimetral 1901, CEP 66077530, Belém, PA, Brazil, §School of GeoSciences, University of Edinburgh, Drummond Street, Edinburgh, UK, ¶Departamento de Meteorologia, Centro de Geociências, Universidade Federal do Pará, Avenida Augusto Correa s/n, Guamá, CEP 66075900, Belem, PA, Brasil

Abstract

In the next few decades, climate of the Amazon basin is expected to change, as a result of deforestation and rising temperatures, which may lead to feedback mechanisms in carbon (C) cycling that are presently unknown. Here, we report how a throughfall exclusion (TFE) experiment affected soil carbon dioxide (CO_2) production in a deeply weathered sandy Oxisol of Caxiuanã (Eastern Amazon). Over the course of 2 years, we measured soil CO_2 efflux and soil CO_2 concentrations, soil temperature and moisture in pits down to 3 m depth. Over a period of 2 years, TFE reduced on average soil CO_2 efflux from $4.3 \pm 0.1\,\mu mol\,CO_2\,m^{-2}\,s^{-1}$ (control) to $3.2 \pm 0.1\,\mu mol\,CO_2\,m^{-2}\,s^{-1}$ (TFE). The contribution of the subsoil (below 0.5 m depth) to the total soil CO_2 production was higher in the TFE plot (28%) compared with the control plot (17%), and it did not differ between years. We distinguished three phases of drying after the TFE was started. The first phase was characterized by a translocation of water uptake (and accompanying root activity) to deeper layers and not enough water stress to affect microbial activity and/or total root respiration. During the second phase a reduction in total soil CO_2 efflux in the TFE plot was related to a reduction of soil and litter decomposers activity. The third phase of drying, characterized by a continuing decrease in soil CO_2 production was dominated by a water stress-induced decrease in total root respiration. Our results contrast to results of a drought experiment on clay Oxisols, which may be related to differences in soil water retention characteristics and depth of rooting zone. These results show that large differences exist in drought sensitivity among Amazonian forest ecosystems, which primarily seem to be affected by the combined effects of texture (affecting water holding capacity) and depth of rooting zone.

Keywords: Brazil, carbon dioxide production, drought, ENSO, soil moisture, soil respiration, soil temperature, soil texture

Received 17 November 2006; revised version received 19 April 2007 and accepted 17 July 2007

Introduction

In the next few decades, climate of the Amazon basin is expected to change, as a result of regional deforestation and rising global temperatures (Nobre *et al*., 1991; Werth & Avissar, 2002). Several climate scenarios predict a warming trend of 1.5–2.5 °C in annual mean temperature for a large part of the tropics (Hulme & Viner, 1998; Cox *et al*., 2000) and some of these scenarios predict more frequent occurrence of ENSO droughts of increasing severity induced by global warming (Timmermann *et al*., 1999). These changes in climate may lead to feedback mechanisms in global biogeochemical cycles

Correspondence: Edzo Veldkamp, tel. + 49 551 397339, fax + 49 551 393310, e-mail: eveldka@gwdg.de

that are presently unknown. For example, climate changes may affect C stocks in vegetation as well as shifts in total soil C and belowground C allocation (Davidson *et al*., 2004).

One-third of the global soil C storage (to 3 m depth) is in the upper metre of tropical soils (Jobbagy & Jackson, 2000). Moreover, a large portion of the soil organic C (SOC) in tropical soils has a short residence time (Amundson, 2001), which implies a high potential for rapid changes in soil C stocks (Trumbore *et al*., 1995). Increasing temperature may therefore lead to additional carbon dioxide (CO_2) release, especially in the tropics (Trumbore *et al*., 1996). Until the early 1990s C fluxes in soil below 1 m depth were often thought to be insignificant compared with C fluxes in the upper metre (e.g. Sombroek *et al*., 1993). However, many forest soils in the Brazilian Amazon are very deep, strongly weathered and contain significant living root biomass below 1 m depth (Nepstad *et al*., 1994). For these Amazonian ecosystems (but also e.g. for deeply weathered forest soils in Costa Rica) it has been shown that significant amounts of labile SOC exists in the subsoil and that between 7% and 17% of total CO_2 efflux at the soil surface originated below 1 m depth (Davidson & Trumbore, 1995; Veldkamp *et al*., 2003; Schwendenmann & Veldkamp, 2006).

Given the projected intensification of ENSO events, which may lead to an increasing frequency of droughts and higher temperatures, an experiment was set up in which throughfall was experimentally reduced to create an artificial drought (Fisher *et al*., 2006). Manipulation of soil moisture availability by experimental reduction of throughfall has been done in temperate forest ecosystems (Borken *et al*., 2003; Hanson *et al*., 2003). Our experiment was part of the Large Scale Biosphere Atmosphere Experiment in Amazon (LBA). Using this throughfall exclusion (TFE) experiment, our goal was to study how an artificially imposed drought affects depth and amount of soil CO_2 production and transport in a deeply weathered soil of the Eastern Amazon. Our hypothesis is that soils with lower capacity to maintain water in the root zone (smaller difference between field capacity and wilting point) will be more promptly affected by reduced precipitation. A similar experimental rainfall manipulation was implemented in another site in Eastern Amazon, Santarém (Nepstad *et al*., 2002). In this experiment, the TFE of three rainy seasons did not lead to significant differences in soil CO_2 efflux (Davidson *et al*., 2004). However, within the Amazon region there is a great diversity of soils and vegetation thus different responses to drought may be expected (Sombroek, 1966). Over the course of 2 years, we monitored soil CO_2 efflux and soil CO_2 concentrations, soil temperature and soil moisture in pits down to 3 m depth in a sandy Oxisol. Using a simple one-dimensional gas diffusion model, which was calibrated using naturally occurring ^{222}Rn profiles, we calculate CO_2 production with depth and we relate this to a range of environmental controls that can potentially affect the production and emission of CO_2 in the soil.

Material and methods

Study site

The experimental site was located in Caxiuanã National Forest, Para, Brazil, (1°43′3.5″S, 51°27′36″W). The forest is a lowland *terra firme* rainforest. Mean annual rainfall is 2272 mm, with a pronounced dry season, when on average only 555 mm of rainfall occurs (Fisher *et al*., 2006). Months with more than 100 mm rainfall were assigned to the wet season (December to June), and the dry season consisted of the period of months with <100 mm rainfall (July to November).

The studied soil is a yellow Oxisol (Brazilian classification: Latosol), which has a broken ironstone layer (0.3–0.4 m thick) at 3–4 m depth. On average, the top 0.5 m of the soil contains 75% sand, 15% clay and 10% silt (Table 1), while the soil deeper than 5 m contains 90% sand, 5% clay and 5% silt. Mineralogy of the clay fraction is dominantly Kaolinite while the sand fraction consists mainly of quartz (Ruivo & Cunha, 2003). The location of the experiment is about 15 m above river level, and during wet season, the water table has been observed at a depth of 10 m (Fisher *et al*., 2006). The forest contains on average 434 trees ha^{-1}. Basal area is 23.9 $m^2\,ha^{-1}$ and leaf area index (LAI) is 5.2 $m^2\,m^{-2}$ (D. Metcalfe, unpublished data).

Experimental design

The experiment consisted of two plots of 1 ha (100 m × 100 m), one control plot and one experimental TFE plot. Both plots were located about 800 m north of the research station. In the TFE plot, a roof of transparent plastic sheeting and wooden guttering was installed at approximately 2 m height above the soil, with the purpose of displacing part of the throughfall from the plot to impose an artificial drought. Both control and the TFE plots were trenched to a depth of 1 m around their borders to reduce the lateral flow of water in roots and soil across plot boundaries. TFE started in January 2002; about 50% of the rainfall was excluded from the soil of the TFE plot. During the peak of the dry season (from mid-September to mid-November) only 50% of the plastic panels were left on the TFE plot in order to have a better aeration under the covered area. At each plot four pits (0.8 m × 1.8 m with 5 m depth) were

Table 1 Chemical and physical properties of the soil of our study area in Caxiuana, Para, Brazil

Depth (cm)	Clay (%)	Silt (%)	Sand (%)	pH H_2O	ECEC ($cmol\,dm^{-3}$)	Total *P* ($mg\,dm^{-3}$)	Total C** ($g\,kg^{-1}$)	Total N ($g\,kg^{-1}$)	C/N
Control									
0–10	18	5	77	4.0	4.4	3.0	9.1	0.4	22.7
10–25	21	6	73	4.1	4.3	1.8	8.8	0.4	22.0
25–50	19	8	73	4.2	4.4	1.2	5.2	0.4	13.7
50–100	22	10	68	4.4	2.8	1.0	5.1	0.4	13.8
100–200	28	9	63	4.5	2.0	0.6	4.0	0.3	12.5
200–300	20	10	70	4.6	1.4	0.7	4.9	0.3	15.8*
TFE									
0–10	13	4	83	4.0	5.2	3.1	11.7	0.3	35.4
10–25	15	7	78	3.0	4.3	2.3	10.1	0.3	33.7
25–50	20	10	70	4.1	3.2	1.2	6.7	0.4	18.6
50–100	23	9	68	4.3	2.7	0.7	4.1	0.3	12.8
100–200	26	10	64	4.4	2.0	0.5	4.9	0.3	16.3
200–300	20	10	70	4.7	1.4	0.5	6.1	0.3	21.8*

*The high C/N ratio observed at 200–300 cm depth may be due to an accumulation of carbon in the broken ironstone layer at 3–4 m depth present in the study site.
Root biomass profile for these plots can be found in Fisher *et al.* (2007).
**Total C and total N include organic plus inorganic C and N.
TFE, throughfall exclusion; C, carbon; N, nitrogen.

established at randomly chosen locations. The plots were further divided into four quadrants in order to facilitate the systematic placement of soil CO_2 efflux chambers.

Measurements of soil CO_2 efflux

Sixteen respiration chambers were deployed systematically forming a cross in the TFE and control plot of the drought experiment, four at each quadrant. Systematic sampling was chosen to cover the plots uniformly. In June 2001, polyvinyl chloride (PVC) rings (0.296 m in diameter, 0.20 m tall) were inserted to a depth of about 0.02 m into the soil. Once inserted, the rings were left in place throughout the time investigated. Rings were kept free of seedlings throughout the whole study period. Dynamic, closed chambers were used to determine soil CO_2 efflux (Sotta *et al.*, 2006). Average chamber volume was about 13 L. Flux chambers were closed with a PVC cover for about 5 min. Air was circulated at a flow rate of about $0.8\,L\,min^{-1}$ between an infrared CO_2 gas analyser (LI-6262; Li-Cor Inc., Lincoln, NE, USA) and the flux chambers. To prevent pressure differences between chamber and atmosphere, chambers were vented to the atmosphere through a 0.25 m long stainless-steel tube (3.2 mm outer diameter). CO_2 concentrations were recorded at 5 s intervals with a datalogger (Campbell CR10X; Campbell Scientific Inc., Logan, UT, USA). CO_2 flux ($\mu mol\,CO_2\,m^{-2}\,s^{-1}$) was calculated from the linear change in CO_2 concentration multiplied by the density of air and the ratio of chamber volume to soil surface area. Air density was adjusted for air temperature measured at the time of sampling. A linear increase in CO_2 concentration usually occurred between 2 and 4 min after placing the cover over the ring. The coefficient of determination (r^2) of the regression was typically better than 0.99. The infrared gas analyser was calibrated in the lab using a loop with a column with CO_2 scrubber (soda lime indicating 4–8 mesh) as zero-standard and a secondary CO_2 standard (510 ppm). The secondary CO_2 standard was calibrated against primary standards from the LBA project.

Each plot was measured every 2 weeks from December 2001 to November 2002 and monthly from December 2002 to November 2003. It took 2 days to measure both plots. All measurements were conducted between 8:00 and 14:00 hours local time. For each plot, the average CO_2 efflux rate was calculated from the 16 chamber flux measurements on a sampling day. Daily mean soil efflux for each plot was calculated by linear interpolation between sampling dates. Daily CO_2 flux rates were then summed up to estimate annual flux rates. Soil temperature at 0.05 m depth was measured with a thermocouple probe (HI 93551; Hanna Instruments, Ann Arbor, MI, USA) and soil water content (SWC) was measured with a soil moisture probe (CS 615, Campbell Scientific Ltd., Lougborough, UK).

Measurements of CO_2 concentration profiles

In December 2001, all eight pits were instrumented for sampling of soil air. Stainless-steel gas sampling tubes (3.2 mm outer diameter) were inserted horizontally at 0.10, 0.25, 0.50, 1.00, 2.00 and 3.00 m depth. The tubes were perforated at one end and closed with a septum holder with septum at the other end to allow sampling of soil air (Davidson & Trumbore, 1995). Tubes at depths of 0.10–1.00 m were 0.90 m long; tubes at greater depth were 1.80 m long. Samples at 0.05 m depth were collected using a 0.10 m stainless-steel tubing adapted to a syringe, which was vertically inserted in the top soil every sampling date. Soil air samples were collected in polypropylene syringes, which were closed with a three-way stopcock. Before a sample was taken, 10–20 mL of soil air was withdrawn and discarded.

Gas samples were analysed for CO_2 concentration in the lab within 8 h using a gas chromatograph (GC 11; Delsi Instruments, Suresnes, France) with a thermal conductivity detector (TCD). Soil air CO_2 concentration was calculated by comparison of integrated peak areas of samples with standard gases (0.051% and 3% CO_2), which were used to make a two-point calibration. The coefficient of variation for replicate injections of standard gases was $<1\%$. Storage tests indicated that on average 9–12% of CO_2 was lost between time of sampling and analysis. Soil CO_2 concentration measurements were made in all pits every 2 weeks in 2002 and monthly in 2003.

Measurements of soil radon activity and radon production

To validate the gas diffusion model, we measured ^{222}Rn activity and ^{222}Rn production rates as described by Davidson & Trumbore (1995). Soil air samples were withdrawn from the stainless-steel gas sampling probes to determine soil air ^{222}Rn concentration (also called radon activity). Soil air (90–120 mL) was dried using a $CaCl_2$ column and introduced into pre-evacuated 150 mL scintillation cells (110A Lucas Cell; Pylon Electronics Inc., Ottawa, ON, Canada). Impulses were measured using a Pylon AB-5 radiation monitor (Pylon Electronics Inc.). Radon production rates were measured for each site and depth interval individually, for both dry and wet conditions following the procedure described by Davidson & Trumbore (1995).

Calculation of CO_2 production

The diffusive properties of a soil media are usually characterized by means of relative diffusion coefficient D_s/D_o. D_s is the diffusion coefficient of a gas in soil air and D_o is the diffusion coefficient of the same gas in free air at standard conditions, (i.e. 0.158 $cm^2 s^{-1}$ for CO_2 at 20 °C and standard pressure of 1013 hPa; Mason & Monchick, 1962). The gas diffusion coefficient in soil (D_s) is a fraction of the gas diffusion coefficient in free air (D_o), as diffusivity depends not only on gas pressure and temperature but also on the amount of air-filled pores and on their continuity and shape. The relationship between D_s/D_o, and soil properties have been investigated in multiple studies and several empirical formulas have been developed to describe soil gas diffusivity. In our experiment, we tested the gas diffusion models with three different approaches:

(a) the model described by Millington & Quirk (1961) for nonaggregated media,

$$\frac{D_s}{D_o} = a^{2x}\left(\frac{a}{\varepsilon}\right)^2, \quad (1)$$

where a is the air-filled porosity ($m^3 m^{-3}$), ε the total porosity ($m^3 m^{-3}$).

(b) the model developed by Millington & Shearer (1971) for aggregated media,

$$\frac{D_s}{D_o} = \left[\frac{\left(\frac{a_{ra}}{\varepsilon_{ra}}\right)^2\left(\frac{a_{ra}}{1-\varepsilon_{er}}\right)^{2x}(1-\varepsilon_{er}^{2y})(a_{er}-a_{er}^{2z})}{\left(\frac{a_{ra}}{\varepsilon_{ra}}\right)^2\left(\frac{a_{ra}}{1-\varepsilon_{er}}\right)^{2x}(1-\varepsilon_{er}^{2y})+(a_{er}-a_{er}^{2z})}\right] + \left[a_{er}^{2z}\left(\frac{a_{er}}{\varepsilon_{er}}\right)^2\right], \quad (2)$$

where a_{ra} is the intra-aggregated air-filled pore space ($m^3 m^{-3}$), ε_{ra} the intra-aggregated total pore space ($\varepsilon_{ra} = \theta_W$ at field capacity), a_{er} the interaggregated air-filled pore space ($m^3 m^{-3}$), ε_{er} the interaggregated total pore space ($\varepsilon_{er} = \varepsilon - \varepsilon_{ra}$) ($m^3 m^{-3}$), x the determined from the relation $a^{2x} + (1-a)^x = 1$ ($m^3 m^{-3}$), y the exponent usually between 0.6 and 0.8 and z the exponent usually between 0.6 and 0.8. and

(c) the model described by Moldrup *et al*. (2000) based on the soil water characteristic curve,

$$\frac{D_s}{D_o} = (2a_{100}^3 + 0.04a_{100})\left(\frac{a}{a_{100}}\right)^{2+3b}, \quad (3)$$

where a_{100} is the air-filled porosity at -100 cm H_2O (porosity with the soil tension at -10 kPa) ($m^3 m^{-3}$), b the pore-size distribution characterized by the slope of the line determined from the water retention curve, which is: $\log -\psi = a + b\theta$, where ψ is the water potential and θ is volumetric water content.

To calculate gas diffusivity we estimated total porosity (ε) from measurements of bulk density and an assumed particle density of 2.65 $Mg m^{-3}$. Air-filled porosity (a) was calculated by the difference between total porosity and water-filled porosity (θ). Water-filled porosity is the volumetric SWC determined from the Time Domain Reflectometry (TDR) probes on a given sampling date. For the aggregated soil model the pore

space is divided into intra-aggregated porosity (estimated from volumetric water content at field capacity) and interaggregated porosity (calculated as the difference between total porosity and volumetric water content at field capacity).

A one-dimensional gas diffusion model developed by Schwendenmann & Veldkamp (2006) was used to predict ^{222}Rn activity throughout the soil profile. Input parameters are measured radon production rates and the diffusion coefficient calculated by the three approaches. These predicted values were compared with measured ^{222}Rn activities from the profile to test the diffusion models for their applicability. The estimated diffusion values from the Millington & Quirk (1961) soil model (M&Q) provided best agreement with the observed ^{222}Rn activities (Fig. 1). Millington & Shearer (1971) model overestimated diffusivity resulting in an underestimation of ^{222}Rn activities, while Moldrup *et al.* (2000) model underestimated diffusivity which resulted in an overestimation of ^{222}Rn activities. Sandy soils normally have a weak aggregation and we speculate that the high sand content of the soil caused the M&Q model (that does not account for soil aggregation) to perform better than the other models. We thus decided to use the M&Q model to estimate gas diffusion coefficients for Caxiuanã soils. Fluxes of CO_2 were estimated at each sampling depth, based on Fick's law (Uchida *et al.*, 1997).

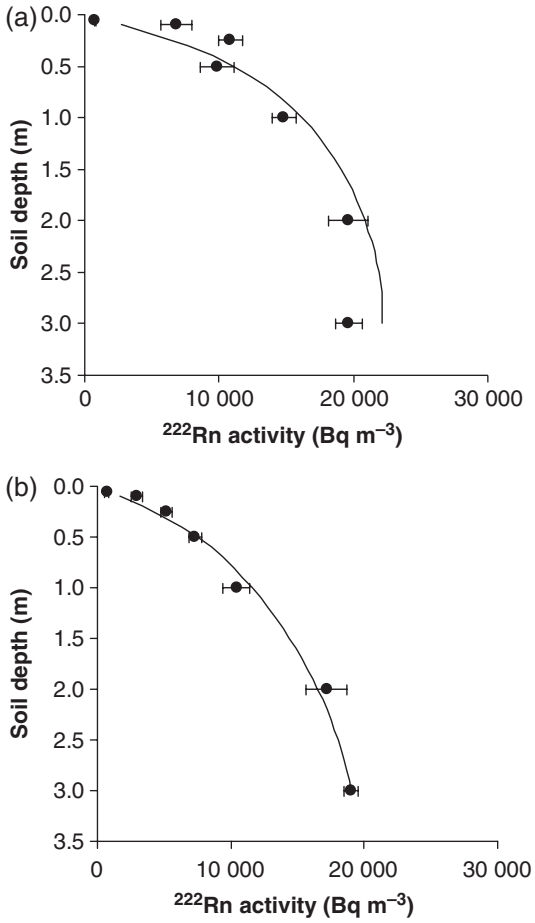

Fig. 1 Depth profiles of simulated and measured radon activity in (a) control and (b) TFE plots. Solid lines (—) show the calculated values using the Millington and Quirk (1961) model. The closed circles (•) are the measured radon activity, where each point is the mean (± standard error) of four profiles. TFE, throughfall exclusion.

Because a uniform diffusion coefficient in the soil is unlikely, a multibox model was used (Davidson & Trumbore, 1995) to calculate soil CO_2 production (P_{CO2}). CO_2 production was calculated for each 0.1 m layer, but as the P_{CO2} rate for these individual layers may not be reliable, we summed the P_{CO2} estimates for larger depth intervals (0.5–1.0, 1.0–2.0 and 2.0–3.0 m; Schwendenmann & Veldkamp, 2006). For the topsoil (0–0.5 m depth) CO_2 production was estimated as the difference between the measured soil CO_2 efflux and the sum of the CO_2 production rates for all individual 0.1 m layers between 0.6 and 3.0 m (subsoil) on a given date. This approach avoids negative production values, in case soil constituents are not uniformly distributed and the soil CO_2 gradient near the surface is not smooth (Davidson & Trumbore, 1995).

Additional measurements

Soil thermocouples sensors were installed at the same depths as the air sampling tubes by attaching them to the perforated end of the air-sampling tubes. Soil temperature was measured using thermocouple T-probes (Omega Engineering, Stamford, CT, USA) read with a handheld thermocouple meter (HI 93551 Microprocessor K, J, T-Type Thermocouple Thermometer; Hanna Instruments Deutschland GmbH, Kehl/Rhein, Germany). At 0.05 m depth the temperature was measured with a T-type thermocouple penetration tip probe (HI 766 Thermocouple probe, Hanna Instruments GmbH).

For soil moisture monitoring, TDR sensors (Soil Moisture Corp, Santa Barbara, CA, USA) were installed vertically at the soil surface (0–0.30 m depth) and horizontally at 0.50, 1.00, 2.00 and 3.00 m depth (Fisher *et al.*, 2007). TDR probes were inserted 1.5 m into the walls, with connections sticking out of the repacked soil wall. Soil moisture measurements were made manually at the time of soil air sampling. Water retention curves of intact soil cores were determined on pressure plates by Dr E. J. M. Carvalho in the soil physics laboratory of Embrapa Amazonia Oriental in Belém, Brazil. The water retention curve for each plot was used to transform SWC in soil water potential (SWP) (ψ). Half-hourly air temperature, photosynthetically

active radiation (PAR) and rainfall were measured by a tower-based automatic weather station in the vicinity of the study site (Carswell *et al*., 2002).

From November 2001 to November 2003, litter was collected monthly, put in paper bags and dried in a ventilated oven for 48 h at 80 °C. The material was separated into three fractions: (a) leaves, (b) twigs and (c) reproductive organs (flower, fruit and seeds); and weighed.

Statistical analyses

Repeated measures ANOVA was used to examine differences in season and treatment. Significant effects were determined at $P < 0.05$. Simple linear regression analysis was used to examine relationships between CO_2 production rates and environmental variables. All statistical analyses were carried out using the STATISTICA 6 software package (StatSoft Inc., Tulsa, OK, USA).

Results

Magnitude and seasonality of soil CO_2 efflux and CO_2 production

The coefficient of variation of soil CO_2 efflux among soil chambers within plots was on average 23% for control plot and 26% for TFE plot, and typically ranged from 13% to 40%. The 2-year average CO_2 efflux rates were higher ($P < 0.01$) for the control plot ($4.3 \pm 0.1\,\mu mol\,CO_2\,m^{-2}\,s^{-1}$) than the TFE ($3.2 \pm 0.1\,\mu mol\,CO_2\,m^{-2}\,s^{-1}$; Fig. 2a). Although the CO_2 efflux of the control plot did not differ significantly between wet season ($4.2 \pm 0.2\,\mu mol\,CO_2\,m^{-2}\,s^{-1}$) and dry season ($4.5 \pm 0.1\,\mu mol\,CO_2\,m^{-2}\,s^{-1}$), we detected strong intraseasonal changes in soil CO_2 efflux. At the onset of the rainy season, soil CO_2 efflux was high, and tended to decrease during the course of the wet season when SWC increased. This was especially clear during the first year. CO_2 efflux in the TFE plot differed significantly ($P < 0.001$) between wet ($3.7 \pm 0.1\,\mu mol\,CO_2\,m^{-2}\,s^{-1}$) and dry season ($2.6 \pm 0.1\,\mu mol\,CO_2\,m^{-2}\,s^{-1}$). During the wet season the TFE did not differ ($P > 0.05$) from the control plot; however, during the dry season CO_2 efflux from the TFE was lower than the control ($P < 0.01$).

The importance of the topsoil (0–0.5 m) for soil CO_2 production (P_{CO2}) is illustrated by the following numbers: between 71% and 73% of soil CO_2 production in both plots occurred within the top 0.5 m of the soil including the forest litter layer. In the topsoil (0–0.5 m including litter layer) the TFE ($2.3 \pm 0.1\,\mu mol\,CO_2\,m^{-2}\,s^{-1}$) had a significantly lower CO_2 production than the control plot ($3.1 \pm 0.1\,\mu mol\,CO_2\,m^{-2}\,s^{-1}$; Fig. 3a). At the onset of the dry season in July 2002 CO_2 production at 0–0.5 m in the TFE plot decreased by approximately 0.8 μmol $CO_2\,m^{-2}\,s^{-1}$. CO_2 production in this layer in the TFE plot dropped by another $0.8\,\mu mol\,CO_2\,m^{-2}\,s^{-1}$ between August and September 2002. Production of CO_2 in the subsoil (0.6–3.0 m depth) in both plots was on average $0.8\,\mu mol\,CO_2\,m^{-2}\,s^{-1}$. During the first 2 months of TFE (February to March 2002) the P_{CO2} between 0.6 and 2.0 m depth was significantly higher in the TFE plot as compared with the control plot ($P < 0.05$; Fig. 3b). Higher P_{CO2} was also observed in the 2.1–3.0 m layer of the TFE plot in the subsequent months (May to June 2002; Fig. 3c). During the dry season there was no difference in P_{CO2} between plots at the subsoil (0.6–3.0 m depth).

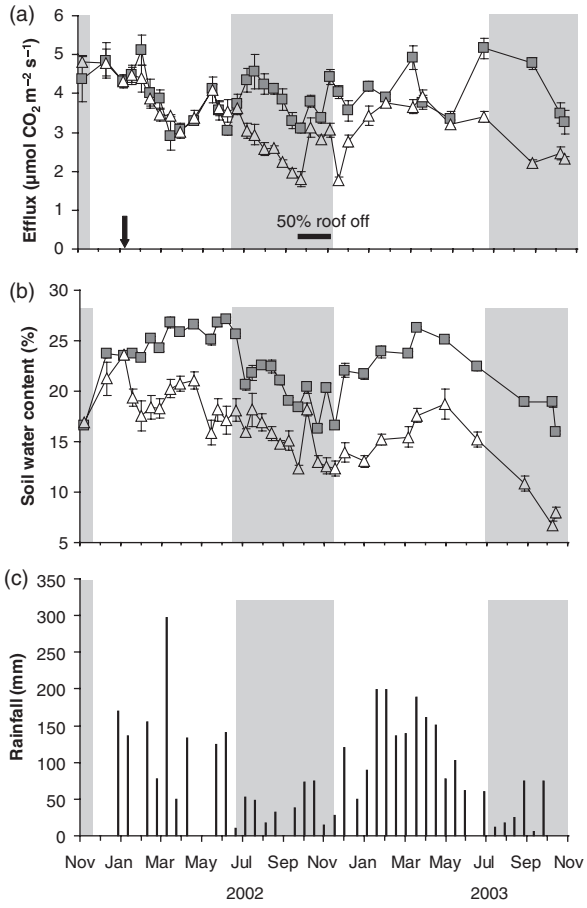

Fig. 2 Temporal variation of (a) soil CO_2 efflux, (b) soil water content (SWC) at 0.3 m depth in control (–■–) and throughfall exclusion (TFE) (–△–) plots and (c) biweekly rainfall from November 2001 to November 2003. Each point is the mean (±standard error) of 16 chambers per treatment. Shaded area mark the dry season and white background indicates wet season. The arrow shows when the TFE began.

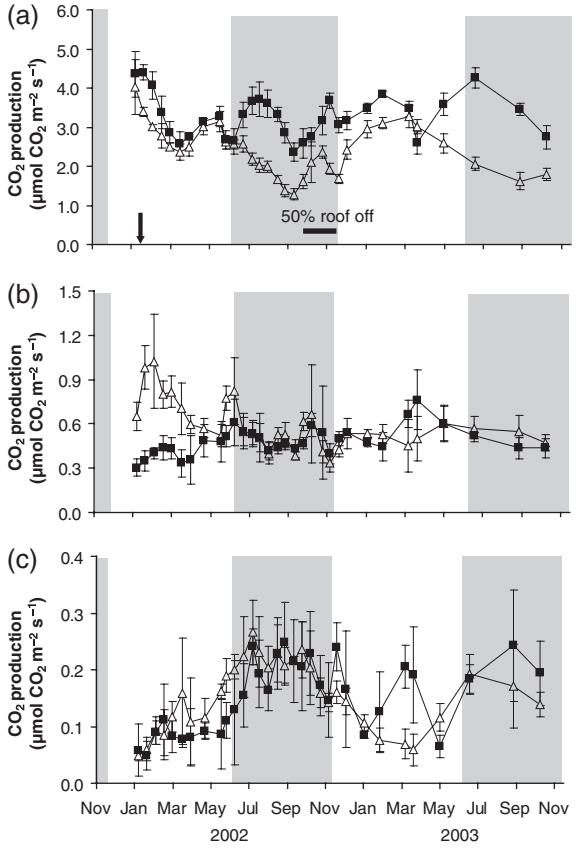

Fig. 3 Temporal variation in carbon dioxide (CO_2) production rates from January 2002 to November 2003 in both control (– ■ –) and TFE (–△–) plot. (a) CO_2 production of the 0–0.5 m layer; (b) CO_2 production of the 0.6–2.0 m layer; and (c) CO_2 production of the 2.1–3.0 m layer. Each point is the average (± standard error) of four profiles. Shaded area mark the dry season and white background indicates wet season. The arrow shows when the throughfall exclusion began.

In the control plot, soil CO_2 production at 0–0.5 m depth was negatively correlated ($r = -0.45$, $P < 0.01$) to 0.6–3.0 m CO_2 production for the whole experiment, which suggests a compensation of CO_2 production in deeper soil layers when CO_2 production decreased because of water stress in the top soil and *vice versa*. The same was not observed for the TFE plot. Nonetheless, the P_{CO2} at 2.1–3.0 m depth in the TFE plot did have a negative correlation ($r = -0.70$, $P < 0.000$) with the P_{CO2} of the top 0.5 m. The contribution of subsoil (0.6–3.0 m) to the total soil CO_2 efflux was higher in the TFE plot (28%) compared with the control plot (17%, $P < 0.000$; Table 2), and it did not differ between seasons and years.

Soil CO_2 concentrations

Soil CO_2 concentration profiles (at 0–3.0 m depth) changed with season in both TFE and control. CO_2 concentrations increased over the course of the wet season and decreased soon after the beginning of the dry season (Fig. 4a and b). Up to 2% CO_2 were measured in the upper layers (0.05 and 0.10 m depth; Fig. 5) of control plot during periods of high precipitation and high SWCs. This observation corroborates with our observations of soil CO_2 efflux, which tends to be lower towards the end of the wet season (Fig. 2a). During the 2-year period the average soil CO_2 concentration measured in the control plot (3.2%) was higher than the concentration in the TFE (1.0%). CO_2 concentration at 0–0.5 m depth in the control plot was three times higher than in the TFE plot, while at 0.6–3.0 m depth the concentration of the control was double the concentration in the TFE plot.

Table 2 Contribution of the subsoil (0.6–3.0 m depth) to the CO_2 efflux by seasons for both plots

Relative contribution of deep soil (%)	2002		2003	
	Wet season	Dry season	Wet season	Dry season
Control plot	16^A	19^A	19	17^A
TFE plot	27^B	32^B	20	31^B

Letters indicate difference between treatments (ANOVA, $P < 0.05$).
TFE, throughfall exclusion; CO_2, carbon dioxide.

Environmental parameters

SWC at 0–0.3 m depth differed between plots ($P < 0.01$). The 2-year average for the control plot was 22.4 ± 0.6% and for TFE was 16.2 ± 0.6% (Fig. 2b) with a calculated corresponding SWP of −47 ± 8 and −201 ± 29 kPa, respectively. In the control, SWP reached a maximum of −184 kPa in the dry season and a minimum of −8 kPa in the wet season, while in the TFE plot SWP varied between −744 kPa in the dry and −22 kPa in the wet season. At the onset of the dry season in July 2002, SWP at 0–0.5 m decreased in the TFE plot from −200 to −319 kPa, and between August and September 2002 it further decreased to −640 kPa (Fig. 4a). During the first 2 months of TFE (February to March 2002) the SWP between 0.6 and 2.0 m depth was −68 kPa lower in the TFE plot as compared with the control plot ($P < 0.05$, Fig. 4b). SWC was also significantly different for control and TFE at all depths in the soil profile and throughout the year. We did not observe differences in soil temperature at 0.05 m depth between control (23.9 ± 0.2 °C) and TFE plot (24.0 ± 0.2 °C), nor at greater depth in the soil profile. Total fine root biomass (< 5 mm diameter) in the 0–0.50 m layer recorded in October 2002 was not

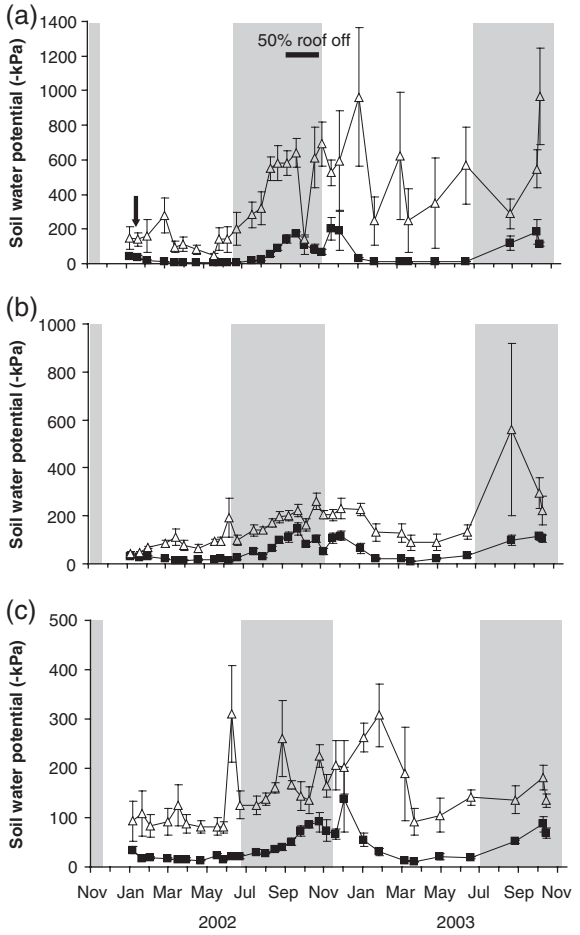

Fig. 4 Temporal variation in soil water potential from January 2002 to November 2003 in both control (–■–) and TFE (–△–) plot. (a) Soil water potential of the 0–0.5 m layer; (b) soil water potential of the 0.6–2.0 m layer; and (c) soil water potential of the 2.1–3.0 m layer. Each point is the average (± standard error) of four profiles. Shaded area mark the dry season and white background indicates wet season. The arrow shows when the throughfall exclusion began.

different between control ($13.9 \pm 1.3\,Mg\,ha^{-1}$) and TFE plot ($15.2 \pm 2.1\,Mg\,ha^{-1}$).

Effects of environmental parameters on soil CO_2 efflux and on CO_2 production

For both control and TFE plot, the relationship between soil CO_2 efflux and SWP (at 0–30 cm depth) could be described with a parabolic function ($r^2 = 0.43$, $P < 0.001$). The shape of the curves from both plots was complementary (Fig. 6a) with the higher water potential from the TFE plot and lower from the control. Taking only the values from the TFE plot, we observed a linear relationship between SWP and CO_2 efflux ($r^2 = 0.36$, $P < 0.001$). We did not find an effect of temperature on soil CO_2 efflux, but there was a positive covariation between soil temperature and SWP ($r^2 = 0.07$, $P < 0.05$; Fig. 6b).

Total litter biomass for both plots had a significant polynomial relationship with soil CO_2 efflux ($r^2 = 0.13$, $P < 0.05$) which is probably explained by the positive linear relationship between total litter and SWC ($r^2 = 0.25$, $P < 0.001$). The reproductive part of the litter (~15% of total litter biomass) also had a high correlation with soil CO_2 efflux and covaried with SWC. A positive linear correlation was found between reproductive part of the litter and SWC for the TFE plot ($r^2 = 0.35$, $P < 0.01$), but for the control plot this linear relationship was negative and only marginally significant ($r^2 = 0.16$, $P = 0.05$).

For the control plot at 0–0.5 m and 0.6–1.0 m depth there was no correlation between P_{CO2} and any other variable. At 1.1–2.0 m depth soil temperature correlated positively with P_{CO2} ($r = 0.41$), while at 2.1–3.0 m depth SWC ($r = -0.52$), soil temperature ($r = 0.41$) and PAR ($r = 0.46$) correlated with P_{CO2}. For the TFE plot at 0–0.5 m depth SWC ($r = 0.63$) and soil temperature ($r = -0.35$) correlated with P_{CO2}. At 0.6–1.0 m SWC ($r = 0.41$), and soil temperature ($r = -0.44$) also had significant correlations with P_{CO2}. P_{CO2} rate at 1.1–2.0 m depth did not correlate with any variable but P_{CO2} rate at 2.1–3.0 m depth did correlate with SWC ($r = -0.48$) and PAR ($r = 0.47$).

Discussion

Effects of seasonality on soil CO_2 emission and production

Although on average no difference was detected in soil CO_2 efflux between dry and wet season, this masks the strong intraseasonal response that we observed as a result of changes in soil moisture content (Fig. 2). The low soil CO_2 efflux at the end of the wet season corresponded with high CO_2 concentrations in the topsoil (Fig. 5), which suggests that low gas diffusivity may have contributed to the low soil CO_2 efflux. A similar pattern in soil CO_2 efflux during the wet season in Costa Rica was also explained with reduced gas diffusivity (Schwendenmann *et al.*, 2003). However, as was the case in Costa Rica, this cannot be the only explanation as soil CO_2 *production* rates (calculated with the gas diffusion model) in the top 0.5 m of our study were also reduced at the end of the wet season (Fig. 3). The high water content at the end of the wet season may have reduced microbial activity and root activity, which may have resulted in lower CO_2 production. Reduced soil CO_2 efflux from an Amazonian forest during the wet season has also been attributed to lower solar flux

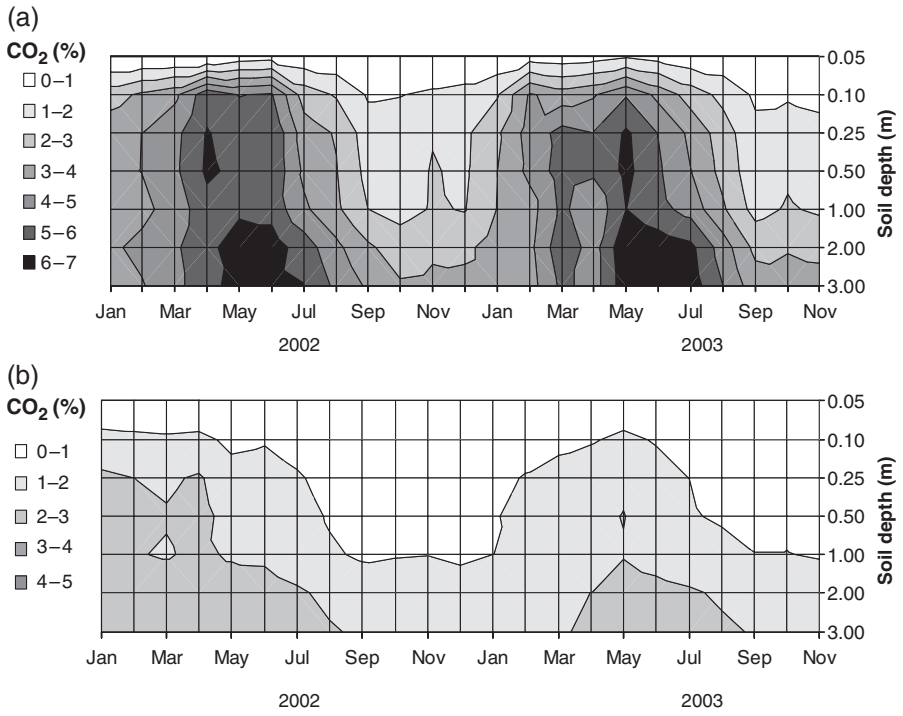

Fig. 5 Isopleths of carbon dioxide (CO_2) concentration in soil air as a function of soil depth and time in (a) control and (b) TFE plot. Each measurement is the mean of four profiles per plot. TFE, throughfall exclusion.

rates, which could affect photosynthesis rates and indirectly also root respiration (Wofsy *et al*., 1988).

At the beginning of the dry season, the observed increase in soil CO_2 efflux corresponded with a strong decrease in CO_2 concentrations (Figs 2a and 5) in the control plot. A similar increase in CO_2 efflux has been observed in a study in Paragominas (Davidson *et al*., 2000) and in Costa Rica (Schwendenmann *et al*., 2003). The increase may be the result of CO_2 diffusing out of the soil that had accumulated during the wet season. However, the transition of wet to dry season may also have caused increased root growth as has been observed (e.g. in a Panamanian rainforest; Cavelier *et al*., 1999). We attribute the decrease in soil CO_2 efflux during the dry season to water stress, which may have reduced root respiration, as well as heterotrophic respiration. Such a decrease has been observed in the forest in Paragominas which has also a strong dry season (Davidson *et al*., 2000) but not in Costa Rica, which has a very weak dry season (Schwendenmann *et al*., 2003). This analysis is also consistent with the negative correlation between P_{CO2} and SWC in control as well as in TFE plot (indicating the high dependency of soil CO_2 production on SWC) and the positive correlation between P_{CO2} and PAR at depth observed for the control plot (indicating the influence of the solar radiation on soil CO_2 production). A strong increase in CO_2 production after some rainstorms at the beginning of the wet season was probably caused by the effect of rewetting. During rewetting normally a soil CO_2 efflux peak occurs which depends on the amount of decomposable SOC (Franzluebbers *et al*., 2000). Field experiments in temperate forests have shown that this CO_2 peak occurs within minutes of rewetting and strongly depends on the amount of rain added to the ecosystem (Borken *et al*., 2003).

Effects of TFE on soil CO_2 efflux and CO_2 production

During the first year, we were able to distinguish three drying phases in the TFE plot. The first phase started with a reduction in soil CO_2 production in the 0.0–0.5 m depth interval shortly after throughfall was excluded (Fig. 3a) which was accompanied by an increase in the depth interval 0.5–2.0 m until May 2002 (Fig. 3b) and in the depth interval 2.0–3.0 m depth from March until July 2002 (Fig. 3c). These features can be explained by a translocation of water uptake (and accompanying root activity) to deeper layers in the TFE plot. This is indicated by the corresponding reduction in SWP throughout the depth profiles (Fig. 4). In the depth interval 2.0–3.0 m depth sufficient water was available

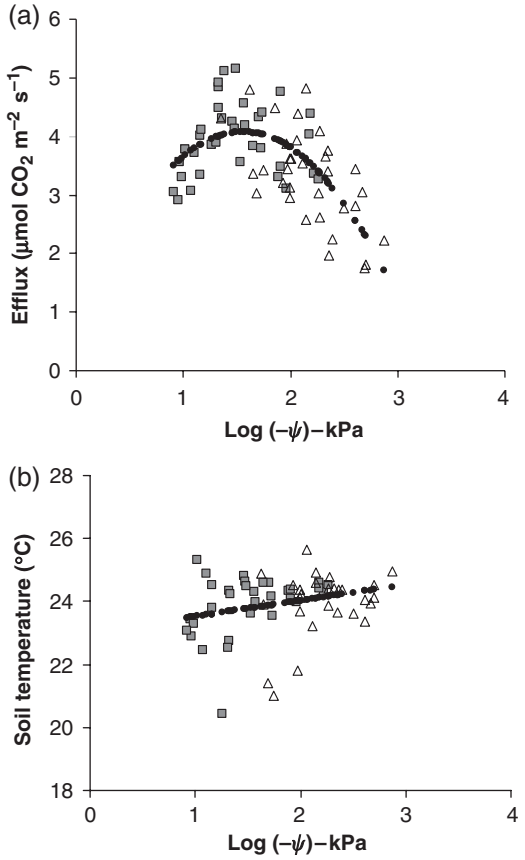

Fig. 6 Relationship between (a) soil water potential at 0.3 m depth and soil carbon dioxide efflux and (b) between soil water potential at 0.3 m depth and soil temperature at 0.05 m depth with data from both control (■) and TFE (△) plot. The regression equation for (a) is Efflux = −1.3664 (log ψ)^2 + 4.2622 (log ψ) + 0.7486 ($r^2 = 0.43$, $P < 0.001$) and for (b) is soil temperature = 0.5051 (log ψ) + 23.008 ($r^2 = 0.07$, $P < 0.05$).

until the beginning of the dry season, when SWP started to decrease, indicating a more intensive use of the water at this depth. Roots will respond to reduced water availability in the topsoil by searching for water deeper in the soil profile (Joslin *et al*., 2000). Our interpretation is further supported by the lack of difference between total soil CO_2 efflux between TFE and control in this period (Fig. 2a) which suggests that there was not yet enough water stress to affect total microbial activity and/or total root respiration. A similar translocation of root activity to deeper layers has been observed in a Costa Rican rain forest even though the dry season in this forest is very weak (Schwendenmann & Veldkamp, 2006). It should be mentioned that in our methodology to derive CO_2 production in the top 0.5 m, CO_2 production in topsoil and subsoil are not completely independent so these results should be interpreted with care.

The second phase of the drying started at the onset of the dry season (July 2002; Fig. 3a). The observed reduction in total soil CO_2 efflux and soil CO_2 production (0–0.5 m) in the TFE plot compared with the control was probably related to a reduction of the activity of soil and litter decomposers, which are sensitive to water stress (Lavine *et al*., 2004; Li *et al*., 2005). At this moment a reduction in total root respiration did not yet occur because sap flow measurements from this period in the TFE plot did not show a reduction suggesting that water stress was not yet severe enough to affect photosynthesis (Fisher *et al*., 2007). Further support comes from an ancillary experiment where we showed that during the wet season about 25% of the soil CO_2 efflux originated from the litter layer, a contribution which became negligible during the dry season (Sotta *et al*., 2006). Bacterial activity declines sharply as water potential falls from −50 to −300 kPa and is negligible at −1500 kPa (Wong & Griffin, 1976). In our experiment, the decrease in soil CO_2 efflux in July 2002 was accompanied with a drop in SWP from −200 to −319 kPa. The lag between the start of the TFE and the reduction in soil CO_2 production and CO_2 efflux was probably related to the time necessary for the litter to dry out. In a temperate forest, Salamanca *et al*. (2003) showed that after 12 months of partial TFE, litter mass loss was not different from the control. However, 3 months of total exclusion resulted in lower litter mass loss, lower CO_2 efflux and lower microbial biomass of decomposing forest litter.

The third phase of drying was characterized by a continuing decrease in soil CO_2 production between August and September 2002 which was probably dominated by a water stress-induced decrease in total root respiration when SWP dropped from −319 to −640 kPa. This is supported by a decline in sap flow which was probably caused by the reduced stomatal conductance due to the low soil-to-leaf water supply (Fisher *et al*., 2007). The reduction in stomatal conductance caused a decrease in estimated gross primary production (GPP) suggesting a reduction in the photosynthetic supply (Fisher *et al*., 2007). This may also explain the high observed correlation between the reproductive parts of the litter and CO_2 efflux.

Comparison with the drought experiment in Santarém and consequences for drought sensitivity

In the control plot (no TFE) the annual estimate of soil CO_2 efflux in Santarém was about 30% lower (10 Mg C ha^{-1} yr^{-1}, Davidson *et al*., 2004) than the estimate for Caxiuanã (15 Mg C ha^{-1} yr^{-1}). The higher soil CO_2 efflux in the control of Caxiuanã may be related to soil texture as the soil CO_2 efflux from an Oxisol with a clay texture in Caxiuanã was also lower compared with the sand (Sotta *et al*., 2006). Apart from soil texture,

rooting depth may have contributed to the difference between the two sites [at least 12 m rooting depth in Santarém (Davidson *et al*., 2004); 10 m rooting depth in Caxiuanã with very low root density under 5 m because of coarse sands (Fisher *et al*., 2007)]. In contrast to our results, 3 years of TFE in Santarém led to a marginal increase of about 9% ($11\,Mg\,C\,ha^{-1}\,yr^{-1}$) in the annual soil CO_2 efflux while in Caxiuanã already the first year of TFE led to a decrease of 22% ($12\,Mg\,C\,ha^{-1}\,yr^{-1}$) in annual soil CO_2 efflux. As the most likely explanation for these different reactions to an induced drought, we hypothesize that in the Santarém experiment more available water is stored in the soil profile than in the Caxiuanã experiment. For Caxiuanã, this would result in a shorter time period needed to reach a matrix potential where decomposition and photosynthesis are strongly reduced because of water stress, and it would explain why, in contrast to Santarém, there was a strong reduction in soil CO_2 efflux in the first year of induced drought. At the moment we can only speculate about the cause of the difference in available water between these sites. Work on soil water retention characteristics from the Brazilian Amazon suggests that clay-rich Oxisols (like in Santarém) do not have higher plant available water (Tomasella & Hodnett, 1998) than the sandier soils at our site (Fisher *et al*., 2007). However, small differences in soil grain size distribution (e.g. fine sand vs. coarse sand or slight differences in clay + silt in a coarse sand) can have a strong effect on soil water retention characteristics. The coarse sand below 5 m depth at Caxiuanã, in combination with very low root biomass at this depth may have affected plant-available water for the whole soil. Identification of the factor(s) that have caused the differences in water storage between Santarém and Caxiuanã is critical because these factors will determine the resilience of Amazonian forests to prolonged dry periods. If our speculation is correct, the texture in the deep subsoil may turn out to be a critical parameter to determine drought sensitively of Amazonian forests.

Acknowledgements

The authors would like to thank the EC Framework 5 Programme, CNPq/DAAD, LBA, and the Museu Paraense Emilio Goeldi for financial and logistical support. Alessandro Rosario helped with the data collection, and we would like to acknowledge two anonymous reviewers who helped to improve the manuscript with their constructive reviews.

References

Amundson R (2001) The carbon budget in soils. *Annual Review of Earth and Planetary Sciences*, **29**, 535–562.

Borken W, Davidson EA, Savage K, Gaudinski J, Trumbore SE (2003) Drying and wetting effects on carbon dioxide release from organic horizons. *Soil Science Society of America Journal*, **67**, 1888–1896.

Carswell FE, Costa AL, Palheta M *et al*. (2002) Seasonality in CO_2 and H_2O flux at an eastern Amazonian rain forest. *Journal of Geophysical Research-Atmospheres*, **107**, 8076, doi: 10.1029/2000JD000284.

Cavelier J, Wright SJ, Santamaria J (1999) Effects of irrigation on litterfall, fine root biomass and production in a semideciduous lowland forest in Panama. *Plant and Soil*, **211**, 207–213.

Cox PM, Betts RA, Jones CD, Spall SA, Totterdell IJ (2000) Acceleration of global warming due to carbon-cycle feedbacks in a coupled climate model. *Nature*, **408**, 184–187.

Davidson EA, Trumbore SE (1995) Gas diffusivity and production of CO_2 in deep soils of the eastern Amazon. *Tellus*, **47B**, 550–565.

Davidson EA, Francoise YI, Nepstad DC (2004) Effects of an experimental drought on soil emissions of carbon dioxide, methane, nitrous oxide, and nitric oxide in a tropical forest. *Global Change Biology*, **10**, 718–730.

Davidson EA, Verchot LV, Cattanio JH, Ackerman IL, Carvalho JEM (2000) Effects of soil water content on soil respiration in forest and cattle pastures of eastern Amazonia. *Biogeochemistry*, **48**, 53–69.

Fisher RA, Williams M, do Vale RL, Lola da Costa A, Meir P (2006) Evidence from Amazonian forests is consistent with isohydric control of leaf water potential. *Plant, Cell and Environment*, **29**, 151–165.

Fisher RA, Williams M, Lola da Costa A, Malhi Y, Costa RF, Almeida S, Meir P (2007) The response of an Eastern Amazonian rain forest to drought stress: results and modelling analyses from a through-fall exclusion experiment. *Global Change Biology*, **13** (Online Accepted Articles), doi: 10.1111/j.1365-2486.2007.01417.x.

Franzluebbers AJ, Haney RL, Honeycutt CW, Schomberg HH, Hons FM (2000) Flush of carbon dioxide following rewetting of dried soil relates to active organic pools. *Soil Science Society of America Journal*, **64**, 613–623.

Hanson PJ, O'Neill EG, Chambers MLS, Riggs JS, Joslin JD, Wolfe MH (2003) Soil Respiration and Litter decomposition. In: *North American Temperate Deciduous Forest Responses to Changing Precipitation Regimes*, Vol. 166 (eds Hanson PJ, Wullschleger SD), pp. 163–189. Springer, New York.

Hulme M, Viner D (1998) A climate change scenario for the tropics. *Climatic Change*, **39**, 145–176.

Jobbagy EG, Jackson RB (2000) The vertical distribution of soil organic carbon and its relation to climate and vegetation. *Ecological Applications*, **10**, 423–436.

Joslin JD, Wolfe MH, Hanson PJ (2000) Effects of altered water regimes on forest root systems. *New Phytologist*, **147**, 117–129.

Lavine MB, Foster RJ, Goodine G (2004) Seasonal and annual changes in soil respiration in relation to soil temperature, water potential and trenching. *Tree Physiology*, **24**, 415–424.

Li YQ, Xu M, Zou XM, Xia Y (2005) Soil CO_2 efflux and fungal and bacterial biomass in a plantation and a secondary forest in wet tropics in Puerto Rico. *Plant and Soil*, **268**, 151–160.

Mason EA, Monchick L (1962) Transport properties of polar-gas mixtures. *The Journal of Chemical Physics*, **36**, 2746–2757.

Millington RJ, Shearer RC (1971) Diffusion in aggregated porous media. *Soil Science*, **3**, 372–378.

Millington RJ, Quirk JM (1961) Permeability of porous solids. *Transactions of the Faraday Society*, **57**, 1200–1207.

Moldrup P, Olesen T, Schjønning P, Yamaguchi T, Rolston DE (2000) Predicting the gas diffusion coefficient in undisturbed soil from soil water characteristics. *Soil Science Society of America Journal*, **64**, 94–100.

Nepstad DC, Carvalho CR de, Davidson EA *et al*. (1994) The role of deep roots in the hydrological and carbon cycles of Amazonian forests and pastures. *Nature*, **372**, 666–669.

Nepstad DC, Moutinho P, Dias-Filho MB *et al*. (2002) The effects of partial throughfall exclusion on canopy processes, aboveground production, and biogeochemistry of an Amazon forest. *Journal of Geophysical Research*, **107**, 8085, doi: 10.1029/2001JD000360.

Nobre CA, Sellers PJ, Shukla J (1991) Amazonian deforestation and regional climate change. *Journal of Climate*, **4**, 957–988.

Ruivo MLP, Cunha ES (2003) Mineral and organic components in archaeological black earth and yellow latosol in Caxiuana, Amazon, Brazil. In: *Ecosystems and Sustainable Development* (eds Tiezzi E, Brebbia CA, Uso JL), pp. 1113–1121. WITT Press, Southampton, UK.

Salamanca EF, Kaneko N, Katagiri S (2003) Rainfall manipulation effects on litter decomposition and the microbial biomass of the forest floor. *Applied Soil Ecology*, **22**, 271–281.

Schwendenmann L, Veldkamp E (2006) Long-term CO_2 production from deeply weathered soils of a tropical rain forest: evidence for a potential feedback to climate warming. *Global Change Biology*, **12**, 1–16.

Schwendenmann L, Veldkamp E, Brenes T, O'Brien JJ, Mackensen J (2003) Spatial and temporal variation in soil CO_2 efflux in an old-growth neotropical rain forest, La Selva, Costa Rica. *Biogeochemistry*, **64**, 111–128.

Sombroek WG (1966) *Amazon Soils: A Reconnaissance of the Soils of the Brazilian Amazon Region*. Centre for Agricultural Publication and Documentation, Wageningen, pp. 120–226.

Sombroek WG, Nachtergaeler FO, Hebel A (1993) Amounts, dynamics and sequestering of carbon in tropical and subtropical soils. *Ambio*, **22**, 417–426.

Sotta ED, Veldkamp E, Guimaraes B, Paixao RK, Ruivo MLP (2006) Landscape and climatic controls on spatial and temporal variation in soil CO_2 efflux in an Eastern Amazonian Rainforest, Caxiuanã, Brazil. *Forest Ecology and Management*, **237**, 57–64.

Timmermann A, Oberhuber J, Bacher A, Esch M, Latif M, Roeckner E (1999) Increased El Nino frequency in a climate model forced by future greenhouse warming. *Nature*, **398**, 694–697.

Tomasella J, Hodnett MG (1998) Estimating soil water retention characteristics from limited data in Brazilian Amazonia. *Soil Science*, **163**, 190–202.

Trumbore SE, Davidson EA, Camargo PB, Nepstad DC, Martinelli LA (1995) Belowground cycling of carbon in forests and pastures of Eastern Amazonia. *Global Biogeochemical Cycles*, **9**, 515–528.

Trumbore SE, Chadwick OA, Amundson R (1996) Rapid exchange between soil carbon and atmospheric carbon dioxide driven by temperature change. *Science*, **272**, 393–396.

Uchida M, Nojiri Y, Saigusa N, Oikawa T (1997) Calculation of CO_2 flux from forest soil using ^{222}Rn calibrated method. *Agricultural and Forest Meteorology*, **87**, 301–311.

Veldkamp E, Becker A, Schwendenmann L *et al*. (2003) Substantial labile carbon stocks and microbial activity in deeply weathered tropical wet forest soils. *Global Change Biology*, **9**, 1171–1184.

Werth D, Avissar R (2002) The local and global effects of Amazon deforestation. *Journal of Geophysical Research*, **107**, 8087, doi: 10.1029/2001JD000717.

Wofsy SC, Harriss RC, Kaplan WA (1988) Carbon dioxide in the atmosphere over the Amazon basin. *Journal of Geophysical Research*, **93**, 1377–1387.

Wong PTW, Griffin DM (1976) Bacterial movement at high matric potentials.1. Artificial and natural soils. *Soil Biology and Biochemistry*, **8**, 215–218.

